DOI: 10.1002/ejoc.200600862

Chiral (–)-DIOP Ruthenium Complexes for Asymmetric Radical Addition and Living Radical Polymerization Reactions

Yusuke Iizuka,[a] Zhaoming Li,[b] Kotaro Satoh,[a] Masami Kamigaito,*[a] Yoshio Okamoto,[c] Jun-ichi Ito,[a] and Hisao Nishiyama[a]

Keywords: Asymmetric catalysis / Radical reactions / Polymerization / Alkenes / Phosphane ligands

A series of ruthenium complexes with chiral phosphane ligands (Ru_2Cl_4[(–)-DIOP]$_3$ (**1**), Ru(Ind)Cl[(–)-DIOP] (**2**), and Ru(Cp*)Cl[(–)-DIOP] (**3**), DIOP = 2,3-(isopropylidenedioxy)-2,3-dihydroxy-1,4-bis(diphenylphosphanyl)butane) were synthesized, characterized by X-ray crystallography, and employed in asymmetric halogen transfer radical addition and metal-catalyzed living radical polymerization reactions of olefins, such as styrene, methyl acrylate (MA), and methyl methacrylate (MMA). X-ray crystallographic analysis revealed the binuclear structure of **1** and the mononuclear structures of **2** and **3**, which suggests that the chiral environments are established around the ruthenium center. Complexes **1** and **2** induced asymmetry in chiral addition reactions with high chemical yield and relatively high optical yield (10–30 % *ee*) for styrene, MA, and MMA, whereas almost no significant chiral induction was observed with the use of **3**. Specifically, the highest *ee* was obtained for **1** with the use of styrene (32 % *ee*) whereas the highest *ee* for **2** was observed with the use of MA (21 % *ee*) and MMA (13 % *ee*). All of the metal complexes induced radical polymerizations of these vinyl monomers in conjunction with a series of haloesters as an initiator. Some systems can control the molecular weights and the terminal groups by the ruthenium-catalyzed reversible activation of the carbon–halogen bond. However, no tacticity control was achieved with all of these DIOP-based ruthenium complexes.

Introduction

Although radical reactions are commonly understood to be notoriously uncontrollable because of the high reactivity of the radical species, recent progresses in controlled and selective radical reactions have changed the understanding and led to many synthetic applications not only for simple low molecular weight compounds, but also for complex natural molecules and polymers with well-defined structures. One of the most effective radical reactions is the atom transfer radical addition (ATRA); this halogen atom transfer is widely employed because of the effectiveness and the synthetic possibilities of halides in the products.[1] These reactions are usually performed between polyhalogen compounds, haloesters, or related halogen compounds and various olefins in the presence of free radical initiators or transition metal catalysts, such as complexes of ruthenium, copper, iron, etc. During the metal-catalyzed halogen transfer reaction, the halogen atom is abstracted by one-electron oxidation of the metal center to form the carbon radical species, which subsequently adds to the carbon–carbon double bond of the olefin. The resulting new carbon-centered radical species receives a halogen atom from the oxidized metal center to form an adduct of the halide and the olefin and to regenerate the reduced original metal complex. Judicious choice of the metals and the ligands results in efficient yields, and can be applied to various reactions and syntheses. The representative metal complexes include $RuCl_2(PPh_3)_3$, CuCl/bipyridine, etc.[2,3]

However, the asymmetric radical addition reactions were rather limited except for a few examples.[4–8] The first relevant metal-catalyzed asymmetric halogen transfer radical addition reactions were reported with chiral ruthenium complexes bearing (+) or (–)-DIOP ligands [DIOP = 2,3-(isopropylidenedioxy)-2,3-dihydroxy-1,4-bis(diphenylphosphanyl)butane], which induced asymmetric radical addition reactions between arenesulfonyl chlorides (RSO_2Cl) and styrenes (CH_2=CHC_6H_4R') to give optically active adducts (20–40 % *ee*) and relatively high chemical yields (40–100 %), both of which were dependent on the substituents (R and R′) and the reaction conditions.[6] The structure of the ruthenium catalyst was proposed to be $Ru_2Cl_4(DIOP)_3$ by IR and ^{31}P NMR spectroscopy[9] although no X-ray crystal structure was obtained. Asymmetric induction was considered to be due to the radicals that were confined in the coordination sphere of the ruthenium complex with a chiral

[a] Department of Applied Chemistry, Graduate School of Engineering, Nagoya University,
Furo-cho, Chikusa-ku, Nagoya 464-8603, Japan
[b] Venture Business Laboratory, EcoTopia Science Institute, Nagoya University,
Furo-cho, Chikusa-ku, Nagoya 464-8603, Japan
[c] EcoTopia Science Institute, Nagoya University,
Furo-cho, Chikusa-ku, Nagoya 464-8603, Japan
Supporting information for this article is available on the WWW under http://www.eurjoc.org or from the author.

ligand, but the mechanism was still unknown. Another precedent result was reported in 1981, in which a rhodium complex with a (–)-DIOP ligand, RhCl[(–)-DIOP], induced the asymmetric addition between bromotrichloromethane (CCl_3Br) and styrene in 32% *ee* and 26% yield although the authors did not suggest a radical reaction.[5] Other asymmetric halogen transfer reactions were finely performed for more complex substrates by using chiral Lewis acids in the presence of a free radical initiator or by using chiral auxiliaries in an olefin to produce enantio- or diastereoselective products, respectively.[4,7,8]

Another recently developed area in controlled radical reactions is the metal-catalyzed living radical polymerization or atom transfer radical polymerization (ATRP) that can precisely control the molecular weights and the terminal groups, which can be further applied to a wide variety of functional materials based on controlled polymer structures. Radical polymerization also relies on metal-catalyzed one-electron redox processes consisting of sequences of halogen-abstraction, radical formation, addition to the double bond of the monomers, and regeneration of the carbon–halogen terminus.[10–14] Although the living radical polymerization reaction was originally reported with the use of $RuCl_2(PPh)_3$, which had been employed for radical addition reactions, developments in polymerization catalysts have now been achieved with more active, effective, and versatile catalysts, such as $Ru(Ind)Cl(PPh_3)_2$ and $Ru(Cp^*)Cl(PPh_3)_2$.[10,15] These evolved features are more or less due to the electron-donating cyclopentadiene (Cp) based η^5-coordinated ligands, which result in lowering the redox potential and increasing the stability of the catalyst. Interestingly, these half-sandwich ruthenium complexes were then employed in low molecular weight radical addition reactions and also proved to be more efficient than the original $RuCl_2(PPh)_3$ catalyst even for radical addition reactions.[16] Therefore, the development of radical polymerization catalysts resulted in the evolution of radical addition catalysts even though the polymerization reaction originated from the radical addition reaction.[10]

The first objective of this study was thus directed to the development of asymmetric radical addition reactions based on a series of chiral ruthenium-DIOP catalysts, $Ru_2Cl_4[(–)\text{-DIOP}]_3$ (**1**), Ru(Ind)Cl[(–)-DIOP] (**2**), and Ru(Cp*)Cl[(–)-DIOP] (**3**) (Scheme 1), among which the latter two complexes were synthesized and characterized by X-ray crystallography for the first time. Although the former DIOP Ru complex (**1**) has already been prepared and employed in asymmetric radical addition reactions with arenesulfonyl chlorides,[6] there were no reported X-ray crystallographic studies and no radical reaction with CCl_3Br. Therefore, we synthesized, isolated, and characterized all of these complexes, used them for the simplest radical addition between CCl_3Br and various olefins, such as styrene, methyl acrylate (MA), and methyl methacrylate (MMA) under the same reaction conditions, and compared the results.

The second objective is to use these chiral ruthenium complexes for metal-catalyzed living radical polymerization reactions and to determine the effects on the molecular weight control and the possibility of stereochemical control during the polymerizations.[17] Although the proposed mechanism for stereochemical induction to the $Ru_2Cl_4[(–)\text{-DIOP}]_3$-catalyzed asymmetric radical addition reaction[6] may suggest a possible stereospecific radical polymerization, no tacticity control was reported by other chiral metal catalysts[18–20] or chiral radical mediators[21] during the living radical polymerization reactions. At present, stereochemical control during the radical polymerizations should rely on other methods with added Lewis acids or with polar solvents, in which these additives or solvents interact with the polar substituents in the monomer and the growing radical species to induce the steric induction.[22,23] The combination of stereospecific radical polymerization

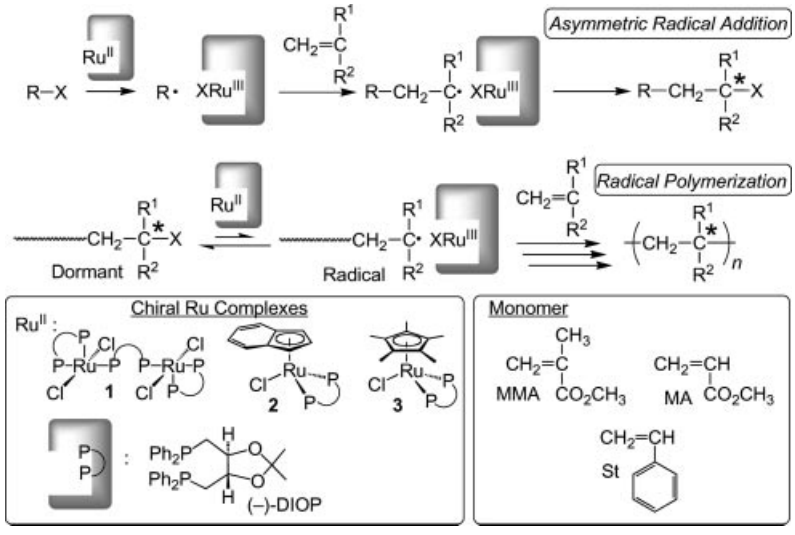

Scheme 1. Chiral (–)-DIOP Ruthenium Complexes for Asymmetric Radical Addition and Living Radical Polymerization.

with living radical polymerization has now proved effective for simultaneous control of the tacticity and the molecular weight of the polymer.[24,25] We herein employed these chiral ruthenium catalysts for the radical polymerizations of MMA, MA, and styrene for the possible simultaneous control of molecular weight and tacticity.

Results and Discussion

Synthesis and Characterization of Chiral Ruthenium Complexes

We first synthesized a series of chiral ruthenium-(–)-DIOP complexes **1**–**3** by a simple ligand exchange reaction[26] between the corresponding triphenylphosphane complexes and (–)-DIOP. As reported in previous papers,[6,9] a phosphane exchange reaction between $RuCl_2(PPh)_3$ and (–)-DIOP at ambient temperature readily yields a neutral green complex, $Ru_2Cl_4[(–)\text{-DIOP}]_3$ (**1**), which can be recrystallized from toluene and *n*-hexane. A similar ligand exchange reaction, but heated at 80 °C, efficiently worked for $Ru(Ind)Cl(PPh)_2$ and $Ru(Cp^*)Cl(PPh)_2$ to yield red-brown crystals of **2** and **3**, respectively.

Figure 1 shows the ^1H NMR spectra ($CDCl_3$, room temp.) of prepared chiral ruthenium complexes **1**–**3**. The spectrum of **1** shows broad signals that are probably due to intramolecular ligand exchange derived from its binuclear structure as already suggested by analysis of the ^{31}P NMR spectra.[9c] On the other hand, a series of sharp peaks are observed in the spectra of **2** and **3** and they can be clearly assigned to the diphosphane ligand (*a*–*d*) and the indenyl (*e* and *f*) or Cp* ring (*g*). The peak intensity ratios of the aromatic protons (*d* and *f*) around 6–8 ppm and the other protons (*a*–*c* and *e* or *g*) between 0.5 and 4.5 ppm suggested that the original Ind- or Cp*-based triphenylphosphane complexes react with the chiral bidentate phosphane in a 1:1 ratio to form **2** or **3**, respectively. The chemical shifts of the peaks *b*, *c*, and *d*, attributable to the chiral diphosphane ligand, are dependent on the Cp-based ligands; this suggests the establishment of asymmetric environments around the Ru center.

The structures of complexes **1**–**3** were further confirmed by X-ray crystallographic analysis of their single crystals, obtained by recrystallization from toluene/*n*-hexane solutions (Figure 2). Table 1 summarizes the selected bond lengths of the chiral ruthenium complexes along with those of the original PPh_3-ruthenium complexes. The bond lengths of Ru–Cl and Ru–Cp′(centroid) in the DIOP complexes are almost the same as those of the corresponding PPh_3 complex and are mainly dependent on the anionic ligand (Cl, Ind, Cp*). The Ru–P bond length in the DIOP complex was slightly shorter than that of the PPh_3 complex.

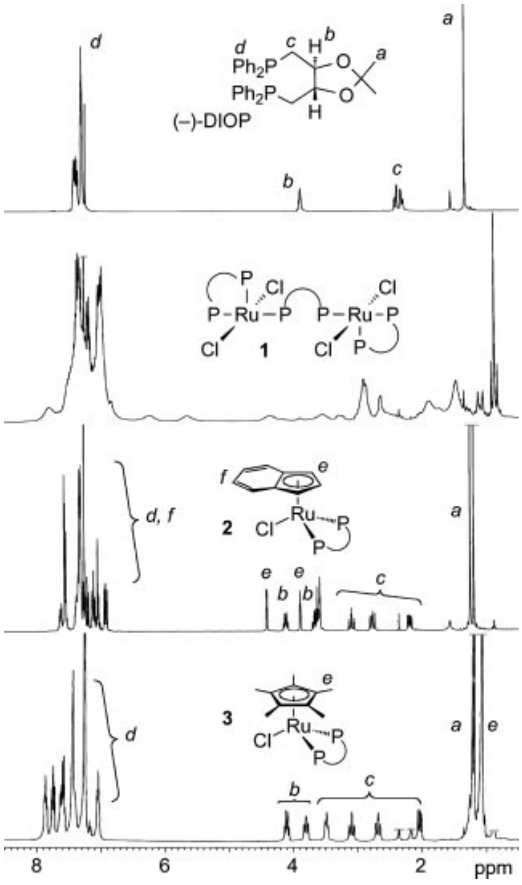

Figure 1. ^1H NMR spectra ($CDCl_3$, 25 °C) of (–)-DIOP and the chiral ruthenium complexes: $Ru_2Cl_4[(–)\text{-DIOP}]_3$ (**1**), Ru(Ind)Cl[(–)-DIOP] (**2**), and Ru(Cp*)Cl[(–)-DIOP] (**3**).

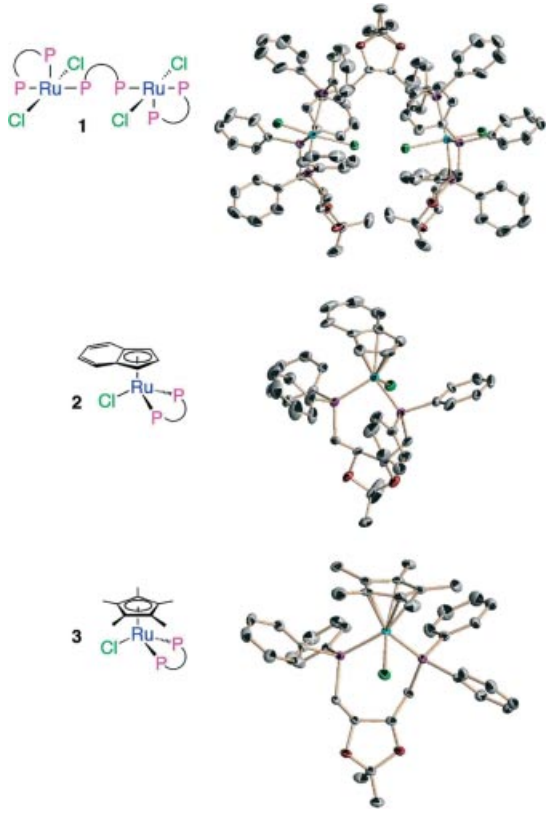

Figure 2. ORTEP diagrams of the chiral ruthenium complexes: $Ru_2Cl_4[(–)\text{-DIOP}]_3$ (**1**), Ru(Ind)Cl[(–)-DIOP] (**2**), and Ru(Cp*)Cl-[(–)-DIOP] (**3**).

Table 1. Selected bond lengths [Å] for ruthenium complexes with estimated standard deviations in parentheses.

	$RuCl_2(PPh_3)_3$[31]	Ru_2Cl_4[(–)-DIOP]$_3$	Ru(Ind)Cl$(PPh_3)_2$[32]	Ru(Ind)Cl(–)-DIOP	Ru(Cp*)Cl$(PPh_3)_2$[33]	Ru(Cp*)Cl(–)-DIOP
Ru–Cl	2.3732(9)	2.3833(8)	2.4370(5)	2.430(2), 2.445(2)	2.4583(6)	2.4470(11)
	2.3916(9)	2.3780(8)	–	–	–	–
Ru–P	2.3557(9)	2.3247(8)	2.2618(5)	2.255(2), 2.2328(19)	2.3379(6)	2.3142(11)
	2.2118(10)	2.1927(8)	2.3306(5)	2.303(2), 2.311(3)	2.3464(5)	2.3162(11)
	2.4334(9)	2.4022(7)	–	–	–	–
Ru–Cp′(cent)	–	–	1.918	1.89(4), 1.91(3)	1.890(3)	1.873(2)

The binuclear structure of Ru_2Cl_4[(–)-DIOP]$_3$ (**1**) has been proposed by IR and ^{31}P NMR spectroscopy and interpreted in terms of a five-coordinate, square pyramidal geometry at each ruthenium atom.[9] This is the first time that the crystal structure of **1** (Figure 2A) proved the bridging structure of the 16-electron complex with a slightly distorted square pyramidal geometry, that is, the bond angle of Cl–Ru–Cl is 155.59° (< 180°). On the other hand, the crystal structures of the Ind- and Cp* complexes showed the neutral 18-electron 1:1 form, Ru(Ind)Cl[(–)-DIOP] (**2**) and Ru(Cp*)Cl[(–)-DIOP] (**3**), with η^5-coordinated indenyl and Cp*-ligands, respectively. The indenyl ring in **2** is slightly slipped toward the unsubstituted carbons (2.167, 2.199, and 2.145 Å) away from the ring-fused carbons (2.340 and 2.377 Å), which indicates a slight distortion of the indenyl ring from η^5- toward η^3-coordination.[27]

Asymmetric Radical Addition with Chiral Ruthenium Complexes

For the estimation of the catalytic activity and asymmetric induction of chiral ruthenium complexes **1**–**3** during the radical addition reaction, they were used in Kharasch addition reactions of bromotrichloromethane (CCl_3Br) to three classes of olefins: styrene, MMA, and MA, which are commonly used as monomers in radical polymerization reactions (Scheme 1).

The three chiral complexes were first examined in the Kharasch addition of CCl_3Br to styrene, in which the reagent concentrations were set at typical conditions for similar additions as follows: [styrene]$_0$ = 1.4 M and [Ru complex]$_0$ = 10 mM in CCl_3Br. Table 2 summarizes the chemical and optical yields of the 1:1 adduct for the Kharasch addition at various temperatures. The chemical and optical yields were confirmed by ^1H NMR spectroscopy and chiral HPLC, respectively (see Experimental Section). With all complexes, and at all temperatures, the reaction smoothly proceeded with a slight induction period to almost quantitatively afford the 1:1 adduct of CCl_3Br and styrene based on the initial amount of styrene, although the reactions were retarded at lower temperatures. All of the chiral complexes preferably provided the (+)-enantiomer, which corresponds to the (*R*)-isomer in absolute configuration.[5] Furthermore, the enantiomeric selectivity with **1** and **2** increased by lowering the temperature, and the adduct obtained with **1** at 0 °C showed the highest enantiomeric excess (32% *ee*) with a high chemical yield (>99%). The optical yield was comparable to that of the rhodium-catalyzed asymmetric addition (32% *ee*), whereas the chemical yield was much higher than that of the Rh-catalyzed reaction (26%).[5] Indenyl ruthenium complex **2** was also effective in asymmetric radical addition reactions, although the activity was lower than that of **1**.

Table 2. Efficiency of chiral ruthenium complexes that mediate the asymmetric radical addition of CCl_3Br to styrene.[a]

Entry	Ru^{II}	Temp. [°C]	Time [h]	Conv.[b] [%]	Yield[c] [%]	*ee*[d] [%]
1	**1**	60	1	>99	>99	21 (+)
2	**1**	40	10	>99	>99	26 (+)
3	**1**	25	30	>99	>99	30 (+)
4	**1**	0	460	>99	>99	32 (+)
5	**2**	60	24	>99	97	15 (+)
6	**2**	40	231	>99	>99	18 (+)
7	**2**	25	1100	75	65	23 (+)
8	**3**	60	24	>99	>99	2 (+)
9	**3**	40	65	>99	99	2 (+)
10	**3**	25	302	>99	>99	1 (+)

[a] Reaction conditions: [styrene]$_0$ = 1.4 M; [Ru^{II}]$_0$ = 10 mM in CCl_3Br. [b] Consumption of styrene determined by ^1H NMR spectroscopy. [c] Chemical yield of the styrene-CCl_3Br 1:1 adduct based on the initial charge of styrene determined by ^1H NMR spectroscopy. [d] The %*ee* values were measured by chiral HPLC (Daicel Chiralcel OJ).

Figure 3 shows a typical example of the kinetic profiles (conversion and chemical yield) of the styrene–CCl_3Br addition reaction at 40 °C (A) and the temperature dependence on the asymmetric selectivity of products with **1**–**3** (B). As shown in Figure 3A, the chemical yields of the adducts were almost the same as the conversions of styrene, which indicates that no side reactions in the radical additions took place. The reaction rate was critically dependent on the complex, and their catalytic activity for the styrene–CCl_3Br reaction was estimated as follows: **1** > **3** > **2**. The differences in the reactivity is most probably dependent on the different bindings of the phosphane and other ligands (Cl, Ind, Cp*). Similarly, the optical yields also changed with the complex and temperature (Figure 3B). The enantiomeric selectivity with **1**–**3** was thus estimated by the thermodynamic evaluation. The difference in the activation enthalpy ($\Delta H^{\ddagger}$) and that of the activation entropy ($\Delta S^{\ddagger}$) between the (+)- and (–)-specific addition can be determined by the appropriate plot of $\ln(P_{(+)}/P_{(-)})$ versus 1/T according to the following equation (1):

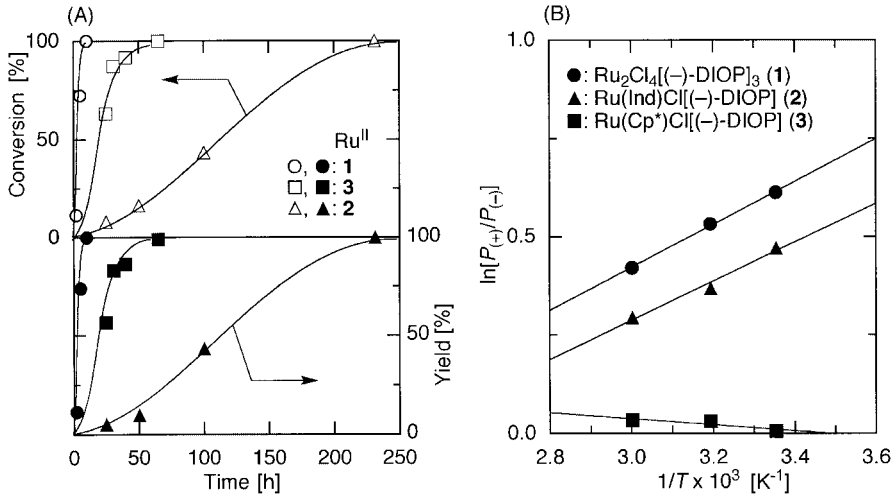

Figure 3. Kinetic profiles at 40 °C (A) and the temperature dependence on the asymmetric selectivity of the products (B) in the asymmetric radical addition of CCl_3Br to styrene with the chiral ruthenium complexes (**1**–**3**): $[styrene]_0$ = 1.4 M; [ruthenium complex] = 10 mM. Ruthenium complex: (○, ●) **1**; (Δ, ▲) **2**; (□, ■) **3**.

$$\ln(P_{(+)}/P_{(-)}) = (\Delta S_{(+)}^{\ddagger} - \Delta S_{(-)}^{\ddagger})/R - (\Delta H_{(+)}^{\ddagger} - \Delta H_{(-)}^{\ddagger})/RT \quad (1)$$

where $P_{(+)}$ and $P_{(-)}$ are the probability, which refers to the fraction of (+)- and (–)-enantiomers in the product, respectively, R is the gas constant (1.987 cal/mol K), and T is the reaction temperature (K). Thus, the slopes of the straight lines in Figure 3 correspond to the contribution of enthalpy to the stereospecificity of the addition reaction. The obtained values of $\Delta H_{(+)}^{\ddagger} - \Delta H_{(-)}^{\ddagger}$ and $\Delta S_{(+)}^{\ddagger} - \Delta S_{(-)}^{\ddagger}$ for the CCl_3Br addition to styrene with **1**–**3** are summarized in Table 3. The negative values of $\Delta H_{(+)}^{\ddagger} - \Delta H_{(-)}^{\ddagger}$ and $\Delta S_{(+)}^{\ddagger} - \Delta S_{(-)}^{\ddagger}$ with **1** and **3** indicate that (+)-specific addition is favored by enthalpy and not favored by entropy, whereas **3** shows a much lower selectivity both in enthalpy and entropy. The slopes obtained with **1** and **2** were almost the same and suggests that the difference in the selectivity is attributed to entropy.

Table 3. Activation parameters for the asymmetric addition with chiral ruthenium complexes 1–3.[a]

Ru^{II}	$\Delta H_{(+)}^{\ddagger} - \Delta H_{(-)}^{\ddagger}$ [cal/mol]	$\Delta S_{(+)}^{\ddagger} - \Delta S_{(-)}^{\ddagger}$ [cal/mol K]
1	–2.42 ± 0.38	–1090 ± 125
2	–2.39 ± 0.37	–987 ± 117
3	0.53 ± 0.36	152 ± 112

[a] The ranges of errors were estimated based on the errors in the determination of *ee* (±0.5% *ee*; see Table 1).

The ruthenium-catalyzed asymmetric radical additions of CCl_3Br were further examined for (meth)acrylic esters, MMA, and MA (Table 4). As for styrene, the addition reactions for both olefins smoothly occurred and the rate was dependent on the catalysts. The chemical yields of the 1:1 adduct were lower than the conversions in most cases; this is attributed to the concurrently occurring polymerization reaction for these (meth)acrylic monomers. However, all these ruthenium catalysts gave optically active 1:1 adducts even for less bulky (meth)acrylates. Among them, indenyl complex **2** gave the highest enantiomeric selectivity for both MMA (13% *ee*) and MA (21% *ee*) even at relatively high temperatures (60 and 40 °C). By lowering the temperature to 25 °C, the reaction with **2** was dramatically retarded and resulted in significantly lower yields of the 1:1 adducts. On the other hand, with a similar 18-electron complex, Ru(Cp*)Cl[(–)-DIOP] (**3**), the optical yield was consistently low (1–2% *ee*) for both MMA and MA, similar to styrene. These results are probably due to the fact that this 18-electron RuCp* complex should release one of the coordinated phosphane atoms upon abstraction of bromine atom from CCl_3Br, which may reduce the enantioselectivity. In contrast, 16-electron ruthenium complex **1** does not need such detaching of the phosphorus moiety. Complex **2** can become an active 16-electron complex by slipping the indenyl ligand from η^5- to η^3-coordination.

Controlled/Living Radical Polymerization with Chiral Ruthenium Complexes

A series of chiral ruthenium complexes were then employed for living/controlled radical polymerizations of styrene, MMA, and MA for possible control of the molecular weight and tacticity. In these polymerizations, a series of α-haloesters (chloride, bromide, and iodide) were employed as the initiator, in which the carbon–halogen bond is activated by the ruthenium complexes to form the initiating and the growing radical species. For the living polymerization reaction with a Ru complex, some additives, such as $Al(OiPr)_3$, are necessary for the enhancement of the rate and the controllability of the polymerization.[10]

We thus investigated the polymerization of styrene with a series of Ru-(–)-DIOP complexes (**1**–**3**) in conjunction with $Me_2C(CO_2Me)CH_2C(CO_2Me)(Me)Cl$ [$(MMA)_2$–Cl] as the initiator in the presence of $Al(OiPr)_3$ as the additive in toluene heated at 100 °C. As shown in Figure 4, the polymerizations of styrene with the chiral complexes proceeded slower

Table 4. Efficiency of chiral ruthenium complexes that mediate the asymmetric radical addition of CCl_3Br to methyl methacrylate and methyl acrylate.[a]

Entry	Olefin	Ru^{II}	Temp. [°C]	Time [h]	Conv.[b] [%]	Yield[c] [%]	*ee*[d] [%]
1	MMA	**1**	60	2	>99	78	7 (–)
2	MMA	**1**	40	7	>99	67	9 (–)
3	MMA	**1**	25	55	>99	72	9 (–)
4	MMA	**2**	60	20	>99	62	13 (–)
5	MMA	**2**	40	170	>99	58	10 (–)
6	MMA	**2**	25	315	27	0.5	n.d.[e]
7	MMA	**3**	60	10	>99	90	1 (–)
8	MMA	**3**	40	55	>99	91	2 (–)
9	MMA	**3**	25	180	>99	99	2 (–)
10	MA	**1**	60	2	99	59	11 (+)
11	MA	**1**	40	8	99	52	11 (+)
12	MA	**1**	25	70	>99	70	15 (+)
13	MA	**2**	60	200	99	78	12 (+)
14	MA	**2**	40	620	95	59	21 (+)
15	MA	**2**	25	520	30	0.6	n.d.
16	MA	**3**	60	24	99	99	2 (+)
17	MA	**3**	40	152	>99	>99	2 (+)
18	MA	**3**	25	370	99	91	1 (+)

[a] Reaction conditions: $[Monomer]_0$ = 1.4 M; $[Ru^{II}]_0$ = 10 mM in CCl_3Br. [b] Consumption of monomer determined by ^1H NMR spectroscopy. [c] Chemical yield of the monomer–CCl_3Br 1:1 adduct based on the initial charge of monomer determined by ^1H NMR spectroscopy. [d] The %*ee* values were measured by chiral HPLC (Daicel Chiralcel OJ). [e] Not determined.

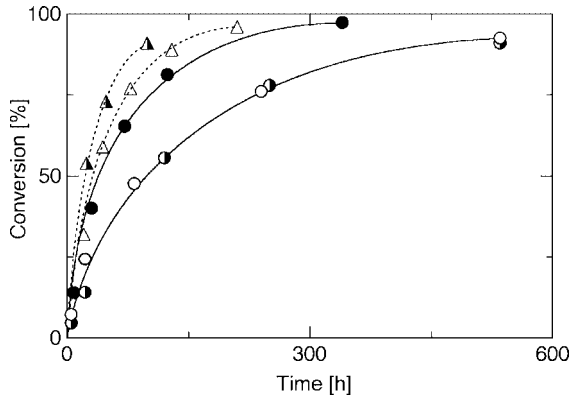

Figure 4. Time-conversion curves of the radical polymerization of styrene with $(MMA)_2$–Cl/ruthenium complex (**1**–**3**) in toluene at 100 °C in the presence of $Al(OiPr)_3$: $[styrene]_0$ = 4.0 M; $[(MMA)_2–Cl]_0$ = 40 mM; [ruthenium complex]$_0$ = 4.0 mM; $[Al(OiPr)_3]_0$ = 40 mM. Ruthenium complex: (●) **1**; (half-solid circle) **2**; (○) **3**; (half-solid triangle) $Ru(Ind)Cl(PPh_3)_2$; (Δ) $Ru(Cp^*)Cl(PPh_3)_2$.

than that those with $Ru(Cp^*)Cl(PPh_3)_2$ under the same conditions. The polymerization rate was dependent on the catalysts in the following order: **1** > **2** ≈ **3**. With all of the complexes, the polymerizations in the absence of $Al(OiPr)_3$ yielded much lower conversions of styrene and lower yields of the polymers.

Figure 5 shows the number-average molecular weights (M_n), polydispersity index (M_w/M_n), and size-exclusion chromatographs (SEC) of the obtained polystyrenes. With binuclear chiral complex **1**, control of the polymer molecular weights was achievable, in which the M_n increased with conversion and was close to the calculated value on the basis of the assumption that one initiator [$(MMA)_2$–Cl] molecule generates one living polymer chain. However, the molecular weight distributions (MWDs) were relatively broad (M_w/M_n ≈ 2.0) throughout the reactions. On the other hand, the DIOP complexes with η^5-coordinated indenyl or Cp* ligands afforded the polymers with an uncontrollable M_n, much higher than the calculated values, and broad MWDs. These results are due to the slow initiation or activation of the initiator and/or the slow interconversion between the active and the dormant species in comparison to the propagation.

The terminal structure of the polystyrene obtained with **1** and $(MMA)_2$–Cl was analyzed by ^1H NMR spectroscopy (Figure 6). In addition to the large absorptions of the main chain repeating units (*d*, *e*, and *f*), the characteristic signals of the initiator moiety (α-end) and the ω-end chloride were observed. Peaks *a* at 0.6–1.1 ppm and *c* at 2.8–3.5 ppm are

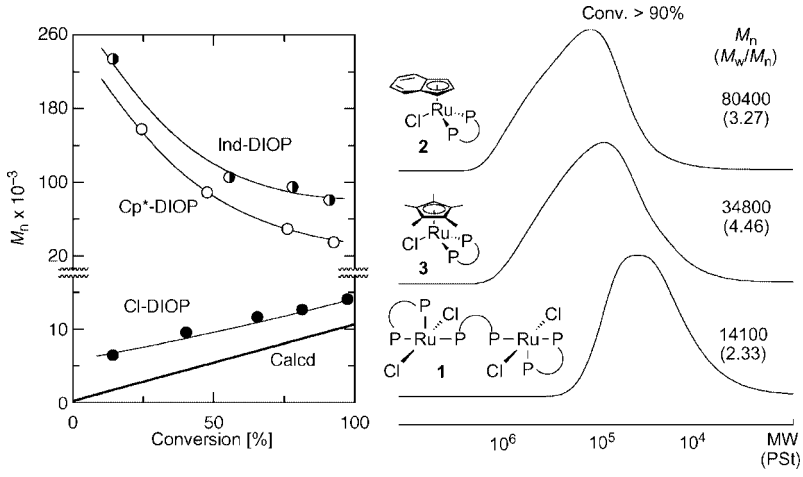

Figure 5. M_n curves and size-exclusion chromatograms of poly(styrene) obtained in the polymerization with $(MMA)_2$–Cl/ruthenium complex (**1**–**3**) in toluene at 100 °C in the presence of $Al(OiPr)_3$: $[styrene]_0$ = 4.0 M; $[(MMA)_2–Cl]_0$ = 40 mM; [ruthenium complex]$_0$ = 4.0 mM; $[Al(OiPr)_3]_0$ = 40 mM. Ruthenium complex: (●) **1**; (half-solid circle) **2**; (○) **3**. The diagonal bold line indicates the calculated M_n assuming the formation of one living polymer per one initiator molecule.

derived from the protons of the methyl groups and methoxy groups at the α-end, respectively. The small absorption *e′* around 4.4 ppm is attributed to the methine proton adjacent to the ω-end chlorine. The M_n obtained from the α-end (*f*/*c*) and ω-end signals (*f*/*e′*) was 5500 and 5100, respectively, which are in good agreement with that by SEC (M_n = 5500) calibrated against polystyrene standard samples. Thus, the number-average end functionality (F_n) was close to unity for both the α- and ω-terminals: $F_n(\alpha)$ = 1.00 and $F_n(\omega)$ = 1.08, where $F_n = M_n(\text{SEC})/M_n(\text{NMR})$. These indicate that $(MMA)_2$–Cl served as the initiator that formed one polystyrene chain per molecule and that all the polymer chains were produced by the activation of the terminal C–Cl bond with **1**.

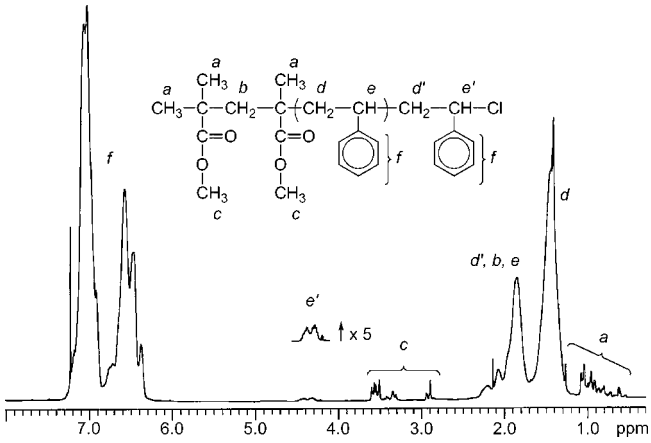

Figure 6. ^{1}H NMR spectrum (400 MHz, $CDCl_3$, 50 °C) of poly(styrene) obtained with $(MMA)_2$–Cl/**1**/Al(O*i*Pr)$_3$ in toluene at 100 °C (M_n = 5,500, M_w/M_n = 2.33).

The tacticity of polystyrene was evaluated by ^{13}C NMR spectroscopy (Figure 7). The steric structure of polystyrene (*mm*:*mr*:*rr* = 24.5:49.8:26.5) obtained with **1** was similar to a typical atactic polystyrene generated by a conventional radical polymerization initiated by AIBN in toluene heated at 100 °C (*mm*:*mr*:*rr* = 25.1:49.4:26.2).[28] Complexes **2** and **3** also resulted in a similar stereochemistry. The tacticity control was thus difficult for the radical polymerization of styrene catalyzed by the chiral ruthenium complexes, though they were effective for the asymmetric radical addition of styrene.

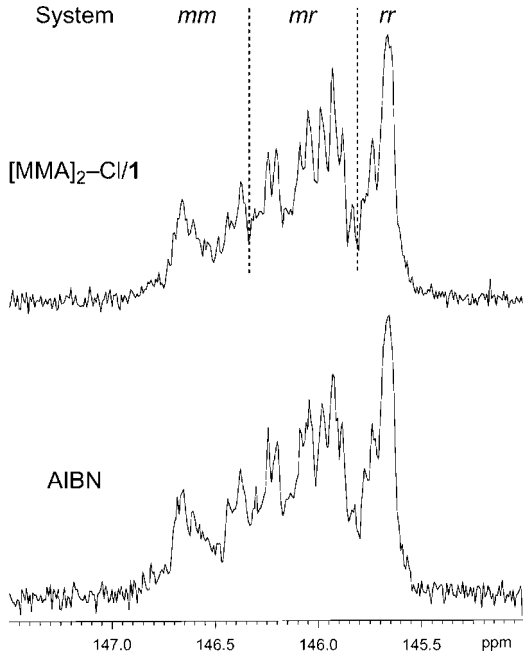

Figure 7. ^{13}C NMR spectra (100 MHz, *o*-dichlorobenzene, 95 °C) of poly(styrene)′s obtained with $(MMA)_2$–Cl/**1**/Al(O*i*Pr)$_3$ (M_n = 14,100, M_w/M_n = 2.33) and α,α-azobisisobutyronitrile (AIBN) in toluene at 100 °C (M_n = 10,800, M_w/M_n = 5.85).

Table 5 summarizes the radical polymerizations of MMA and MA with chiral complexes **1**–**3**, where a series of alkyl halides, $(MMA)_2$–Cl, EMA–Br [$Me_2C(CO_2Et)Br$], and EMA–I [$Me_2C(CO_2Et)I$], were employed as the initiators. For the polymerization of MA with the iodide initiator, all of the M_ns obtained with **1**–**3** were relatively close to the calculated values with the assumption that one molecule of the initiator generates one living polymer chain even though the MWDs were broad. Polymerizations of MA with the bromide and chloride haloesters resulted in higher molecular weights. The iodide initiator produced poly(MMA), the

Table 5. Efficiency of chiral ruthenium complexes that mediated the radical polymerization of methyl methacrylate (MMA) and methyl acrylate (MA).[a]

Entry	Monomer	Ru^{II}	Initiator	Additive	Time [h]	Conv.[b] [%]	M_n(calcd)[c]	M_n(SEC)[d]	M_w/M_n[d]	*mm*/*mr*/*rr*[e] [%]	*m*/*r*[f] [%]
1	MMA	**1**	$(MMA)_2$-Cl	none	270	90	9,300	42,700	2.14	n.d.[g]	n.d.
2	MMA	**1**	EMA-Br	none	500	95	9,700	28,800	1.86	n.d.	n.d.
3	MMA	**1**	EMA-I	none	730	38	4,000	6,400	2.06	n.d.	n.d.
4	MMA	**1**	$(MMA)_2$-Cl	Al(O*i*Pr)$_3$	115	90	9,200	58,300	2.33	n.d.	n.d.
5	MMA	**1**	EMA-Br	Al(O*i*Pr)$_3$	200	96	9,800	41,700	2.30	n.d.	n.d.
6	MMA	**1**	EMA-I	Al(O*i*Pr)$_3$	9	94	9,600	19,900	2.14	3/36/61	21/79
7	MMA	**2**	EMA-I	Al(O*i*Pr)$_3$	155	97	9,900	19,100	6.25	n.d.	n.d.
8	MMA	**3**	EMA-I	Al(O*i*Pr)$_3$	141	92	9,400	18,000	3.78	4/36/60	22/78
9	MA	**1**	EMA-I	Al(O*i*Pr)$_3$	20	94	8,300	10,100	1.69	–	48/52
10	MA	**2**	EMA-I	Al(O*i*Pr)$_3$	140	95	8,400	8,900	1.99	–	48/52
11	MA	**3**	EMA-I	Al(O*i*Pr)$_3$	140	96	8,500	9,100	1.90	–	48/52

[a] Polymerization conditions: $[M]_0/[\mathbf{1}]_0/[Ru^{II}]_0/[Al(OiPr)_3]_0$ = 2000/20/4/40 mM. [b] Determined by GC. [c] M_n(calcd) = MW (M) × $[M]_0/[\mathbf{1}]_0$ × Conv. + MW(**1**). [d] Determined by SEC. [e] Determined by the carbonyl carbon in ^{13}C NMR spectroscopy. [f] Calculated by equation, $r = rr + mr/2$ (for MMA) or determined by the methylene proton in ^{1}H NMR (for MA). [g] Not determined.

molecular weight of which became close to the calculated values with increasing conversion, whereas the MWDs were broader.

The tacticities of poly(MA) and poly(MMA) were then evaluated by ^1H and ^{13}C NMR spectroscopic analysis, respectively. All of the stereochemistries were almost the same as those obtained by conventional radical polymerization. The control of the stereochemistry was also difficult for the MA and MMA polymerizations with these chiral ruthenium complexes. This is probably due to the fact that the chiral ruthenium species do not exist near the growing radical species during the propagation once it abstracts a halogen from the carbon–halogen bond. Thus, chiral induction during the halogen transfer radical addition reaction might not originate from the radicals confined in the coordination sphere of the ruthenium complex,[6] but can rather be ascribed to the chiral ruthenium(III) species that can mediate chiral induction upon giving the halogen atom back to the carbon radical species to form the 1:1 adduct. However, for the radical polymerizations with these ruthenium-(–)-DIOP complexes, all of the obtained polymers showed relatively broad MWDs due to the slow interconversion between the radical and the dormant species. This suggests that successive monomer addition occurs before the radical is again capped with the halogen. Under such conditions, the ruthenium(III) species no longer exists near the growing radical species and cannot control the addition direction of the monomer to the growing radical species. If one can achieve very fast activation and deactivation processes for the carbon–halogen bond, the stereochemistry of the radical polymerization may be possibly influenced by the chiral ruthenium center.

Conclusions

In conclusion, a series of chiral Ru-(–)-DIOP complexes were synthesized, characterized, and employed in halogen transfer radical additions as well as living/controlled radical polymerizations of various vinyl compounds. X-ray crystallographic analysis revealed the binuclear structure of Ru_2Cl_4[(–)-DIOP]$_3$ and the mononuclear structure of Ru(Ind)Cl[(–)-DIOP] and Ru(Cp*)Cl[(–)-DIOP], which suggests that the chiral environments are established around the ruthenium center. The former two complexes induced asymmetric chiral addition reactions in high chemical yields and relatively high optical yields (10–30% *ee*) for styrene, MA, and MMA. However, tacticity control during the radical polymerizations was impossible.

Experimental

Materials: Styrene (Wako; >99%), MMA (Tokyo Kasei; >98%) and MA (Tokyo Kasei; >99%) were distilled from calcium hydride under reduced pressure before use. $RuCl_2(PPh_3)_3$, Ru(Ind)Cl$(PPh_3)_2$, Ru(Cp*)Cl$(PPh_3)_2$ (Wako), and Al(O*i*Pr)$_3$ (Aldrich; >99.99%) were used as received and handled in a glove box (VAC Nexus) under a moisture- and oxygen-free argon atmosphere (O_2 < 1 ppm). (–)-2,3-(Isopropylidenedioxy)-2,3-dihydroxy-l,4-bis(diphenylphosphanyl)butane [(–)-DIOP] (Tokyo Kasei; >97%) was used as received. CCl_3Br (Tokyo Kasei; >98%) and EMA–Br [$Me_2C(CO_2Et)Br$] (Tokyo Kasei; >98%) were distilled from calcium hydride before use. The chloride initiator $(MMA)_2$–Cl [$Me_2C(CO_2Me)CH_2C(CO_2Me)(Me)Cl$] was prepared according to the literature.[29] The iodide initiator EMA–I [$Me_2C(CO_2Et)I$] was prepared by the method of Curran et al.;[30] b.p. 50 °C/9 Torr. *n*-Hexane (Wako; >96%), toluene (Wako; >97%), *n*-pentane (Wako; >96%), and 1,2,3,4-tetrahydronaphthalene (Tokyo Kasei; >98%) were dried overnight with calcium chloride and distilled from sodium benzophenone ketyl before use.

Synthesis of Ru_2Cl_4[(–)-DIOP]$_3$ (1): The reaction was carried out with the use of a syringe under a dry argon atmosphere in an oven-dried glass tube equipped with three-way stopcocks. A heterogeneous mixture of (–)-DIOP (1.78 g, 3.57 mmol) and $RuCl_2(PPh_3)_3$ (1.37 g, 1.43 mmol) was stirred in toluene (56 mL) for 13 h at room temperature. The starting solid material was gradually dissolved to give a homogeneous dark green solution. After the solvent was removed in vacuo, the product was dissolved in toluene (8 mL). Into the solution, *n*-pentane (80 mL) was added slowly to form a green precipitate. The solid was filtered with a cannula with filter paper, washed with *n*-hexane (20 mL × 3), and dried under vacuum. The complex (1.28 g) was obtained as a green powder (97.3%). $C_{93}H_{96}Cl_4O_6P_6Ru_2$ (1839.55): calcd. C 60.72, H 5.26, Cl 7.71; found C 60.84, H 5.17, Cl 7.45. For X-ray crystallographic analysis, the complex (50 mg) was dissolved in toluene (2.0 mL) and recrystallized by the layering of *n*-hexane (15 mL) followed by standing the mixture at room temperature for one week to give a green crystal. X-ray crystallography analysis indicated that one molecule of toluene was contained per molecule of the binuclear complex.

Synthesis of Ru(Ind)Cl[(–)-DIOP] (2): Reaction in analogy to Ru_2Cl_4[(–)-DIOP]$_3$ (**1**) of (–)-DIOP (970 mg, 1.95 mmol) and Ru(Ind)Cl$(PPh_3)_2$ (892 mg, 1.15 mmol) in toluene (20 mL) heated at 80 °C for 8 h gave the product as an orange solid. Yield: 788 mg, 91.4%. $C_{40}H_{39}ClO_2P_2Ru$ (750.21): calcd. C 64.04, H 5.24, Cl 4.73; found C 64.34, H 5.30, Cl 4.63. For X-ray crystallographic analysis, the complex (50 mg) was dissolved in toluene (1.5 mL) and recrystallized by the layering of *n*-hexane (15 mL) followed by standing the mixture at room temperature for one week to give an orange crystal. X-ray crystallography indicated that one molecule of *n*-hexane was contained per two molecules of the disordered complex.

Synthesis of Ru(Cp*)Cl[(–)-DIOP] (3): Reaction in analogy to Ru_2Cl_4[(–)-DIOP]$_3$ (**1**) of (–)-DIOP (1.00 g, 2.01 mmol) and Ru(Cp*)Cl$(PPh_3)_2$ (918 mg, 1.18 mmol) in toluene (28 mL) heated at 80 °C for 8 h gave the product as a yellow solid. Yield: 837 mg, 94.5%. $C_{41}H_{47}ClO_2P_2Ru$ (770.28): calcd. C 63.93, H 6.15, Cl 4.60; found C 64.64, H 6.26, Cl 4.64. For X-ray crystallographic analysis, the complex (50 mg) was dissolved in toluene (1.5 mL) and recrystallized by the layering of *n*-hexane (15 mL) followed by standing the mixture at room temperature for one week to give a yellow crystal.

General Procedure for Asymmetric Radical Addition: All the reactions were carried out with the use of a syringe under a dry argon atmosphere in sealed glass tubes. For a typical example: Styrene (0.29 g, 2.8 mmol), Ru_2Cl_4[(–)-DIOP]$_3$ (**1**, 37 mg, 0.02 mmol), 1,2,3,4-tetrahydronaphthalene (37 mg, 0.28 mmol), and CCl_3Br (1.7 mL) were placed in a dry glass tube. Immediately after mixing, the solution was evenly charged into eight glass tubes, and the tubes were sealed by flame under a nitrogen atmosphere. The tubes were immersed in a thermostatic oil bath heated at 40 °C. In predeter-

mined intervals, the reaction was terminated by the cooling of the reaction mixtures to –78 °C. Monomer conversion and yield of the adduct were determined from concentrations of the residual monomer and adduct measured by ^{1}H NMR spectroscopy with 1,2,3,4-tetrahydronaphthalene as an internal standard. The reaction mixture was evaporated in vacuo and the residue was purified by column chromatography and eluted with pure *n*-hexane. The obtained white solid was analyzed for enantiomer separation by HPLC equipped with a chiral column. All of the products were characterized by ^{1}H and ^{13}C NMR spectroscopy and elemental analysis.

General Procedure for Radical Polymerization: Polymerization was carried out with the use of a syringe under a dry argon or nitrogen atmosphere in sealed glass tubes. A typical example for polymerization of styrene with $(MMA)_2$–Cl/Ru_2Cl_4[(–)-DIOP]$_3$/Al(O*i*Pr)$_3$ is given below: Ru_2Cl_4[(–)-DIOP]$_3$ (**1**, 0.049 g, 0.027 mmol) was dissolved in toluene (3.8 mL). Styrene (1.04 g, 0.01 mol), Al(O*i*Pr)$_3$ (41 mg, 0.2 mmol), and a toluene solution of $(MMA)_2$–Cl (0.1 mL, 0.1 mmol) were then added into the Ru_2Cl_4[(–)-DIOP]$_3$ solution, sequentially in this order. Immediately after mixing, the solution was evenly charged into eight glass tubes, and the tubes were sealed by flame under a nitrogen atmosphere. The tubes were immersed in a thermostatic oil bath heated at 100 °C. In predetermined intervals, the polymerization reaction was terminated by the cooling of the reaction mixtures to –78 °C. Monomer conversion was determined from the concentration of residual monomer measured by gas chromatography with 1,2,3,4-tetrahydronaphthalene as an internal standard. The quenched reaction solutions were washed with HCl (1 M) and water and then evaporated to dryness to give the products, which were subsequently dried overnight for GPC measurement.

Measurements: ^{1}H- and ^{13}C-NMR spectra were recorded with a Varian Gemini 2000 spectrometer (400 and 100 MHz for ^{1}H NMR and ^{13}C NMR, respectively) operating at 50 °C in $CDCl_3$. The triad tacticity of PMMA was determined on the basis of the area of the carbonyl carbon of the side chain and the diad tacticity of PMA was on the basis of the area of the methylene protons of the main chain. The M_n and M_w/M_n of polymers were measured by size-exclusion chromatography in THF at 40 °C on two polystyrene gel columns [Shodex K-805L (pore size: 20–1000 Å; 8.0 mm i.d. × 30 cm) × 2; flow rate 1.0 mL/min] connected to a Jasco PU-980 precision pump and a Jasco 930-RI refractive index detector. The columns were calibrated against eight standard polystyrene samples (Shodex; M_p = 520–900,000; M_w/M_n = 1.01–1.14) for polystyrene and seven standard poly(MMA) samples (Shodex; M_p = 1990–1950000; M_w/M_n = 1.02–1.09) for poly(MMA) and poly(MA). The enantiomeric excess of the products were measured by chiral HPLC in *n*-hexane/2-propanol (98:2 v/v) on cellulose tris-(4-methylbenzoate) columns supported on silica [Daicel CHIRALCEL OJ (4.6 mm i.d. × 25 cm); flow rate 0.5 mL/min] connected to a Jasco PU-980 precision pump, a Jasco UV-970 Intelligent UV/Vis detector, and a Jasco OR-990 polarimetric detector. X-ray data were collected at 173 K for Ru_2Cl_4[(–)-DIOP]$_3$ (**1**), Ru(Ind)Cl[(–)-DIOP] (**2**), and Ru(Cp*)Cl[(–)-DIOP] (**3**) with a Bruker SMART APEX CCD diffractometer with graphite-monochromated Mo-K_α radiation (λ = 0.71073 Å). Cell parameters were refined with 36294, 25981, and 26370 reflections for Ru_2Cl_4[(–)-DIOP]$_3$ (**1**), Ru(Ind)Cl[(–)-DIOP] (**2**), and Ru(Cp*)Cl[(–)-DIOP] (**3**), respectively. The diffraction frames were integrated on the SAINT package. The structures were solved and refined with SHELXTL. CCDC-619361 to -619363 contain the supplementary crystallographic data for this paper. These data can be obtained free of charge from The Cambridge Crystallographic Data Centre via www.ccdc.cam.ac.uk/data_request/cif.

Supporting Information (see footnote on the first page of this article): Crystal data and structure refinement details for complexes **1**–**3**, ORTEP diagrams of complexes of **1**–**3**.

Acknowledgments

This work was supported in part by the 21st Century Program "Nature-Guided Materials Processing" and a Grant-in-Aid for Priority Areas "Advanced Molecular Transformations of Carbon Resources" by the Ministry of Education, Culture, Sports, Science and Technology, Japan. We thank Mr. K. Shiraki and Mr. H. Tsurumoto (Wako Pure Chemical Industries, Ltd.) for providing Ru(Ind)Cl(PPh$_3$)$_2$ and Ru(Cp*)Cl(PPh$_3$)$_2$ and Dr. C. Yamamoto (Nagoya University) for helpful suggestions with chiral HPLC analyses.

[1] a) M. S. Kharasch, E. V. Jensen, W. H. Urry, *Science* **1945**, *102*, 128; b) F. Minisci, *Acc. Chem. Res.* **1975**, *8*, 165; c) J. P. Iqbal, B. Bhatia, N. K. Nayyar, *Chem. Rev.* **1994**, *94*, 519; d) G. van Koten, R. A. Gossage, L. A. van de Kuil, *Acc Chem. Res.* **1998**, *31*, 423–431.

[2] a) H. Matsumoto, T. Nakano, Y. Nagai, *Tetrahedron Lett.* **1973**, *14*, 5147–5150; b) H. Matsumoto, T. Nikaido, Y. Nagai, *Tetrahedron Lett.* **1975**, *16*, 889–902; c) H. Matsumoto, T. Nikaido, Y. Nagai, *J. Org. Chem.* **1976**, *41*, 396–398; d) H. Matsumoto, T. Nakano, K. Takasu, Y. Nagai, *J. Org. Chem.* **1978**, *43*, 1734–1736.

[3] For reviews, see: a) T. Naota, H. Takaya, S. Murahashi, *Chem. Rev.* **1998**, *98*, 2599–2660; b) B. M. Trost, F. D. Toste, A. B. Pinkerton, *Chem. Rev.* **2001**, *101*, 2067–2096; c) N. Kamigata, T. Shimizu, *Rev. Heteroat. Chem.* **1997**, *17*, 1–50; d) K. Severin, *Curr. Org. Chem.* **2006**, *10*, 217–224.

[4] a) D. P. Curran, N. A. Porter, B. Giese, *Acc Chem. Res.* **1991**, *24*, 304–310; b) D. P. Curran, N. A. Porter, B. Giese in *Stereochemistry of Radical Reactions*, Wiley-VCH, Weinheim, **1996**; c) M. P. Sibi, N. A. Porter, *Acc Chem. Res.* **1999**, *32*, 163–171; d) M. P. Sibi, S. Manyem, J. Zimmerman, *Chem. Rev.* **2003**, *103*, 3263–3295.

[5] S. Murai, R. Sugise, N. Sonoda, *Angew. Chem. Int. Ed. Engl.* **1981**, *20*, 475–476.

[6] a) M. Kameyama, N. Kamigata, M. Kobayashi, *Chem. Lett.* **1986**, 527–528; b) M. Kameyama, N. Kamigata, M. Kobayashi, *J. Org. Chem.* **1987**, *52*, 3312–3316; c) M. Kameyama, N. Kamigata, *Bull. Chem. Soc. Jpn.* **1987**, *60*, 3687–3691; d) M. Kameyama, N. Kamigata, *Bull. Chem. Soc. Jpn.* **1989**, *62*, 648–650.

[7] a) M. Gerster, P. Renaud, *Angew. Chem. Int. Ed.* **1998**, *37*, 2562–2579; b) C. L. Mero, N. A. Porter, *J. Am. Chem. Soc.* **1999**, *121*, 5155–5160; c) J. H. Zhang, G. Wu, N. A. Porter, *Tetrahedron Lett.* **1997**, *38*, 2067–2070; d) H. Feng, I. K. Kavrakova, D. A. Pratt, J. Tellinghuisen, N. A. Porter, *J. Org. Chem.* **2002**, *67*, 6050–6054; e) E. J. Enholm, A. Bhardawaj, *Tetrahedron Lett.* **2003**, *44*, 3763–3765.

[8] a) B. Boutevin, E. B. Dongala, *Tetrahedron Lett.* **1977**, *18*, 4315–4316; b) L. A. van de Kuil, Y. S. J. Veldhuizen, D. M. Grove, J. W. Zwikker, L. W. Jenneskens, W. Drenth, W. J. J. Smeets, A. L. Spek, G. van Koten, *Recl. Trav. Chim. Pays-Bas* **1994**, *113*, 267–277; c) V. L. Tararov, T. F. Savel′eva, Yu. T. Struchkov, A. P. Pisarevskii, N. L. Raevskii, Yu. N. Belokon, *Russ. Chem. Bull.* **1996**, *45*, 600–609; d) V. L. Tararov, T. F. Savel′eva, Yu. N. Belokon, *Russ. Chem. Bull.* **1996**, *45*, 610–612.

[9] a) B. R. James, D. K. W. Wang, R. F. Voigt, *J. Chem. Soc., Chem. Commun.* **1975**, 574–575; b) B. R. James, R. S. McMillan, R. H. Morris, D. K. W. Wang, *Adv Chem. Ser* **1978**, *167*, 122–135; c) K. Ohkubo, I. Terada, K. Sugahara, K. Yoshinaga, *J. Mol Catal.* **1980**, *7*, 421–425; d) U. Matteoli, P. Frediani, M. Bianchi, *J. Mol Catal.* **1981**, *12*, 265–319; e) H. Kawano, T. Ikariya, Y. Ishii, T. Kodama, M. Saburi, S. Yoshikawa, Y. Uch-

ida, S. Akutagawa, *Bull. Chem. Soc. Jpn.* **1992**, *65*, 1595–1602.
[10] a) M. Kato, M. Kamigaito, M. Sawamoto, T. Higashimura, *Polym. Prepr Jpn.* **1994**, *43*, 1792–1793; b) M. Kato, M. Kamigaito, M. Sawamoto, T. Higashimura, *Macromolecules* **1995**, *28*, 1721–1723; c) M. Kamigaito, T. Ando, M. Sawamoto, *Chem. Rev.* **2001**, *101*, 3689–3745; d) M. Kamigaito, T. Ando, M. Sawamoto, *Chem. Rec.* **2004**, *4*, 159–175.
[11] a) J.-S. Wang, K. Matyjaszewski, *J. Am. Chem. Soc.* **1995**, *117*, 5614–5615; b) K. Matyjaszewski, J. Xia, *Chem. Rev.* **2001**, *101*, 2921–2990.
[12] V. Percec, B. Barboiu, *Macromolecules* **1995**, *28*, 7970–7972.
[13] C. Granel, Ph. Dubois, R. Jérôme, Ph. Teyssié, *Macromolecules* **1996**, *29*, 8576–8582.
[14] D. M. Haddleton, C. B. Jasieczek, M. J. Hannon, A. J. Shooter, *Macromolecules* **1997**, *30*, 2190–2193.
[15] a) H. Takahashi, T. Ando, M. Kamigaito, M. Sawamoto, *Macromolecules* **1999**, *32*, 3820–3823; b) T. Ando, M. Kamigaito, M. Sawamoto, *Macromolecules* **2000**, *33*, 5825–5829; c) Y. Watanabe, T. Ando, M. Kamigaito, M. Sawamoto, *Macromolecules* **2001**, *34*, 4370–4374; d) T. Shibata, K. Satoh, M. Kamigaito, Y. Okamoto, *J. Polym. Sci: Polym. Chem.* **2006**, *44*, 3609–3615.
[16] a) F. Simal, L. Wlodarczak, A. Demonceau, A. F. Noels, *Tetrahedron Lett.* **2000**, *41*, 6071–6074; b) F. Simal, L. Wlodarczak, A. Demonceau, A. F. Noels, *Eur. J. Org. Chem.* **2001**, 2689–2695; c) L. Quebatte, K. Thommes, K. Severin, *J. Am. Chem. Soc.* **2006**, *128*, 7440–7441.
[17] A. Matsumoto in *Handbook of Radical Polymerization* (Ed. K. Matyjazsewski), Wiley-Interscience, Hoboken, **2002**, pp. 691–773.
[18] a) D. M. Haddleton, D. J. Duncalf, D. Kukulj, A. M. Heming, A. J. Shooter, A. J. Clark, *J. Mater. Chem.* **1998**, *8*, 1525–1532; b) R. M. Johnson, C. Ng, C. C. M. Samson, C. L. Fraser, *Macromolecules* **2000**, *33*, 8618–8628.
[19] a) M. Tsuji, R. Sakai, T. Satoh, H. Kaga, T. Kakuchi, *Macromolecules* **2002**, *35*, 8255–8257; b) M. Tsuji, R. Sakai, T. Satoh, H. Kaga, T. Kakuchi, *Polymer J.* **2003**, *35*, 84–87; c) M. Tsuji, T. Aoki, R. Sakai, T. Satoh, H. Kaga, T. Kakuchi, *J. Polym Sci. Part A: Polym Chem.* **2004**, *42*, 4563–4569.
[20] F. Stoffelbach, P. Richard, R. Poli, T. Jenny, C. Savary, *Inorg. Chim. Acta* **2006**, *359*, 4447–4453.
[21] a) R. D. Puts, D. Y. Sogah, *Macromolecules* **1996**, *29*, 3323–3325; b) R. Braslau, N. Naik, H. Zipse, *J. Am. Chem. Soc.* **2000**, *122*, 8421–8434; c) G. Ananchenko, K. Matyjaszewski, *Macromolecules* **2002**, *35*, 8323–8329; d) E. Drockenmuller, J.-P. Lamps, J.-M. Catala, *Macromolecules* **2004**, *37*, 2076–2083.
[22] S. Habaue, Y. Okamoto, *Chem. Rec.* **2001**, *1*, 46–52.
[23] a) Y. Isobe, D. Fujioka, S. Habaue, Y. Okamoto, *J. Am. Chem. Soc.* **2001**, *123*, 7180–7181; b) S. Habaue, Y. Isobe, Y. Okamoto, *Tetrahedron* **2002**, *58*, 8205–8209; c) Y. Suito, Y. Isobe, S. Habaue, Y. Okamoto, *J. Polym. Sci. Part A: Polym Chem.* **2002**, *40*, 2496–2500; d) Y. Isobe, S. Suito, Y. Habaue, Y. Okamoto, *J. Polym Sci. Part A: Polym Chem.* **2003**, *41*, 1027–1033; e) B. Ray, Y. Isobe, K. Morioka, S. Habaue, Y. Okamoto, M. Kamigaito, M. Sawamoto, *Macromolecules* **2003**, *36*, 543–545; f) B. Ray, Y. Isobe, S. Habaue, M. Kamigaito, Y. Okamoto, *Polym. J.* **2004**, *36*, 728–736; g) B. Ray, Y. Isobe, K. Matsumoto, S. Habaue, Y. Okamoto, M. Kamigaito, M. Sawamoto, *Macromolecules* **2004**, *37*, 1702–1710; h) B. Ray, Y. Okamoto, M. Kamigaito, M. Sawamoto, K. Seno, S. Kanaoka, S. Aoshima, *Polym. J.* **2005**, *37*, 234–237.
[24] a) J.-F. Lutz, D. Neugebauer, K. Matyjaszewski, *J. Am. Chem. Soc.* **2003**, *125*, 6986–6993; b) J.-F. Lutz, W. Jakubowski, K. Matyjaszewski, *Macromol. Rapid Commun.* **2004**, *25*, 486–492.
[25] a) Y. Sugiyama, K. Satoh, M. Kamigaito, Y. Okamoto, *J. Polym. Sci. Part A: Polym. Chem.* **2006**, *44*, 2086–2098; b) M. Kamigaito, K. Satoh, D. Wan, K. Koumura, T. Shibata, Y. Okamoto, *ACS Symp Ser* **2006**, *944*, 26–39; c) M. Kamigaito, K. Satoh, *J. Polym. Sci., Part A: Polym. Chem.* **2006**, *44*, in press.
[26] P. W. Armit, T. A. Stephenson, *J. Organomet. Chem.* **1973**, *57*, C80–C81.
[27] a) J. M. O′Connor, C. P. Casey, *Chem. Rev.* **1987**, *87*, 307–318; b) V. Cadierno, J. Díez, M. P. Gamasa, J. Gimeno, E. Lastra, *Coord. Chem. Rev.* **1999**, *193–195*, 147–205; c) M. J. Calhorda, C. C. Romão, L. F. Veiros, *Chem. Eur. J.* **2002**, *8*, 868–875.
[28] T. Kawamura, N. Toshima, *Macromol. Rapid Commun.* **1994**, *15*, 479–486.
[29] T. Ando, M. Kamigaito, M. Sawamoto, *Macromolecules* **2000**, *33*, 2819.
[30] D. P. Curran, E. Bosch, J. Kaplan, M. Newcomb, *J. Org. Chem.* **1989**, *54*, 1826–1831.
[31] A. R. Cowley, J. R. Dilworth, C. A. Maresca, W. von Beckh, *Acta Crystallogr. Sect. E* **2005**, *61*, m1237–m1239.
[32] M. Kamigaito, Y. Watanabe, T. Ando, 9994–9995.
[33] D. C. Smith Jr, C. M. Harr, L. Luo, C. Li, M. E. Cucullu, C. H. Mahler, S. P. Nolan, *Organometallics* **1999**, *18*, 2357–2361.

Received: October 2, 2006
Published Online: December 8, 2006

